NACA

RESEARCH MEMORANDUM

FLIGHT TESTS OF A TWO-DIMENSIONAL WEDGE DIFFUSER AT TRANSONIC AND SUPERSONIC SPEEDS

By

M. A. Faget

Langley Aeronautical Laboratory
Langley Field, Va.

NATIONAL ADVISORY COMMITTEE FOR AERONAUTICS

WASHINGTON
August 11, 1948

NATIONAL ADVISORY COMMITTEE FOR AERONAUTICS

RESEARCH MEMORANDUM

FLIGHT TESTS OF A TWO-DIMENSIONAL WEDGE DIFFUSER AT TRANSONIC AND SUPERSONIC SPEEDS

By M. A. Faget

SUMMARY

A two-dimensional wedge diffuser, designed to be used with a ducted-airfoil ram jet, was tested on a rocket-powered test vehicle up to a Mach number of 1.45.

Orifice plates and a choking section behind the diffuser exit simulated burning in a combustion chamber by providing the proper pressure drop.

Results obtained from these tests showed there were no abrupt changes in mass flow and pressure recovery as the model velocity increased through the transonic region. Diffuser efficiency, defined as the percent of kinetic energy recovered, was computed to be 95.5 percent at $M = 1.2$. Impact pressures at several points in the diffuser exit indicated that there was a large wake from the island which was used to fair the wedge.

INTRODUCTION

In reference 1 the ducted-airfoil ram jet was proposed as having the advantages of compactness and accessibility of controls in comparison to the ducted-fuselage ram jet, and a theoretical analysis was made that indicated the possibility of high performance for the ducted-airfoil unit. An investigation of the ducted-airfoil ram jet has accordingly been undertaken by the Langley Laboratory of the NACA, and the present paper reports the results of some tests of a small two-dimensional diffuser applicable to the proposed ram-jet installation.

A diffuser with a faired, protruding wedge for external compression was selected for testing, as it was considered the most suitable for use in the ducted-airfoil ram jet. The general considerations in the design of such a two-dimensional diffuser are essentially similar to those for the corresponding three-dimensional diffuser with a protruding cone, which are discussed in reference 2. The central wedge was made sufficiently slender so that the shock wave would be attached at a Mach number of 1.4, corresponding to the estimated top speed of the test vehicle. The gain in pressure recovery for this type of diffuser entrance,

when compared with the converging-diverging type (reference 3), would be small at the design speed of $M = 1.4$. However, some of the data from these tests could be extrapolated to high Mach number designs of the same type.

Flight tests of the diffuser were made on two-stage rocket-powered test vehicles fired at the Pilotless Aircraft Research Test Station at Wallops Island, Va. The technique of flight testing with instrumented models equipped with telemeters made it possible to obtain the pressure recovery and mass flow of the diffuser design in the transonic range and at velocities as high as $M = 1.45$ in the supersonic range.

Description of Apparatus and Tests

Test diffusers.- A cross section of the ducted airfoil, showing the general configuration and significant dimensions of the two-dimensional diffuser tested, is presented in figure 1. The protruding wedge of the diffuser has a half-angle of 9°. This wedge is faired back along the center line of the diffuser forming an island which divides the diffuser into two similar ducts. The wedge half-angle of 9° was selected so that at the design speed of $M = 1.4$ an oblique shock wave would become attached to the wedge. This shock wave would fall ahead of the diffuser entrance. The entrance lips are sharpened and curved to make the inner surfaces of the lips tangent to the streamlines behind the oblique shock wave. After entering the diffuser the air is compressed at subsonic velocities by the expansion of the duct cross section. The expansion angle is $2\frac{3}{4}^\circ$ in the forward portion and increases to 10° at the diffuser exit. Orifice plates and a choking section following the diffuser exit regulate the mass flow through the diffuser. The diffuser is separated from the body of the test vehicle by an open passageway in the ducted airfoil to eliminate the effects of the body boundary layer on the diffuser performance.

A pressure survey was made at the exit of one of the diffusers on the test vehicle. The other diffuser on the test vehicle was not surveyed and was used only to provide aerodynamic balance. The part of the diffuser exit which was surveyed was enclosed between two ribs $3\frac{1}{2}$ inches apart. These ribs ran the full length of the subsonic portion of the diffuser and separated the portion surveyed from the rest of the diffuser. Since this portion was in the center of the semispan, the flow at the entrance to this portion may be considered two dimensional. The diffuser was divided by the island into two channels which were mirror images; therefore, the exit of only one channel was surveyed. Impact pressures were measured at different points in the two models tested with overlapping check points. In the first model the impact pressure was measured at the center line and 0.26 inch, 0.52 inch, and 0.78 inch from the center line, while in the second model impact pressure was measured at the center line and 0.09 inch, 0.18 inch,

and 0.27 inch from the center line. This arrangement was selected to provide the maximum amount of instrumentation in the wake of the island. The pressure-survey tubes, as well as the arrangement of the ribs and orifice plates, are shown in figure 2 which is a photograph of the diffuser during construction.

Test vehicle.- The test vehicle was powered by two 5-inch British Cordite rocket motors arranged in two stages. The general arrangement of the booster and sustainer stages is shown in figure 3. The two ducted airfoils containing two-dimensional diffusers acted as tail surfaces stabilizing the second stage in one plane and conventional tail fins gave the required stability in the other plane. The body of the second stage housed the second-stage rocket motor in the aft end and the instruments and a six-channel telemeter in the forward end. The booster stage consisted of the booster motor with stabilizing fins clamped on the rear end. An attachment mounted on the front of the booster motor held the two stages rigidly together during the boosting period and allowed the two stages to disengage when the booster motor ceased to produce thrust. A time-delay squib fired the sustaining motor soon after the booster dropped free. A photograph of the model and booster on the launching rack is shown in figure 4.

Instrumentation.- A C. W. Doppler radar near the launching site was used to measure velocity of the model during flight. A six-channel telemeter in the nose of the test vehicle was used to transmit the data from four differential pressure cells that measured impact pressures in the diffuser, and two absolute pressure cells that measured the static pressure in the diffuser and the total pressure at the nose of the test vehicle. The total pressure at the nose was to be used to obtain model velocity in case the radar failed to function. However, radar records were good and were used since they are more accurate.

Immediately after each flight a radiosonde balloon was released. This radiosonde provided data from which atmospheric conditions were obtained. High-speed movie cameras tracked the model during flight and timed still cameras gave photographs of the launching. A photograph of a launching from one of the timed still cameras is presented in figure 5.

Tests.- Data from the accelerating part of the flight only were used in calculating the results. This was done because inaccuracies in trajectory calculations and atmospheric conditions reduced from radiosonde-balloon data increased with altitude. In both tests movies from the tracking camera as well as visual observation showed there was very little roll and little or no pitching and yawing during flights, indicating that the diffuser was near zero angle of attack during the tests. The telemeter channel measuring impact pressure at the center line of the diffuser exit failed in the second model. With the exception of this one channel failure, good telemeter records were obtained in both tests.

[redacted]

ANALYSIS OF DATA

The reduced radiosonde-balloon data and Doppler radar data enabled the flight velocity and free-stream conditions to be determined at every point along the model trajectory. The reduced telemeter data made possible the determination of pressure distribution at the diffuser exit. Through the use of compressible-fluid flow relations the Mach number and velocity distribution at the diffuser exit as well as the mass flow were determined throughout the measured flight range of the model.

The diffuser efficiency, defined in reference 2 as the percentage of available kinetic energy recovered in the diffusion process, is expressed by the equation:

$$\eta = 1 - \left(\frac{2}{\gamma - 1}\right)\left(\frac{1}{M_o^2}\right)\left[\left(\frac{H_o}{H_1}\right)^{\frac{\gamma-1}{\gamma}} - 1\right]$$

The diffuser efficiency, defined as the ratio of the rise in static pressure to the loss of impact pressure, is expressed in the equation:

$$\eta = 1 - \frac{H_o - H_1}{q_{c_o} - q_{c_1}}$$

where:

M_o free-stream Mach number

H_o free-stream total pressure

H_1 diffuser-exit total pressure

q_{c_o} free-stream impact pressure

q_{c_1} diffuser-exit impact pressure

The plotted points in figure 6, showing the ratio of diffuser-exit static pressure to free-stream static pressure, are points taken directly from the telemeter record and radiosonde-balloon record for the two tests. The excellent agreement of these points with the faired curve are an indication of the accuracy of the pressure measurements. The data from the telemeter channels used to obtain impact pressure were reduced to Mach number values and plotted against flight Mach number. Values then taken from these curves at even increments of flight Mach numbers were used to plot the Mach number distribution curve (fig. 7).

[redacted]

The curves of average diffuser-exit Mach number and velocity, mass flow, and efficiency were obtained from values taken from the faired curves in figures 6 and 7, and for these curves no experimental points are shown. The average Mach number at the diffuser exit, which was obtained from the Mach number distribution curve, was actually not representative of the whole diffuser. The end effects produced by the boundary layer from the ribs were not taken into account in computing the values for average Mach number at the diffuser exit. This would make the measured values greater than the average values. This error in the average diffuser-exit Mach number would produce an error of the same magnitude in both the diffuser-exit velocity and mass flow. This same error in the diffuser-exit Mach number would also result in an error in the diffuser efficiency although of a low order. For example, decreasing the diffuser-exit Mach number by 5 percent, but keeping the pressure ratio the same, would decrease the efficiency at $M = 1.2$ by less than one-half of 1 percent.

Since these tests were made on different days and since the altitude of the models was continually changing throughout the tests, the curves showing mass flow and diffuser-exit velocity have been corrected to correspond to standard sea-level conditions in the free stream.

RESULTS AND DISCUSSION

The velocity-distribution curves (fig. 7) show that the boundary layer from the shell and the wake from the island extended to the center of the channel. The velocity distribution was about the same for all flight velocities, and no large changes are indicated through the transonic region. However, some tendency for the velocity distribution to flatten with increasing supersonic flight speeds can be noted.

The diffuser-exit Mach number should be expected to reach a maximum value, corresponding to the choking duct exit, and remain near constant at higher flight Mach numbers. It is shown in figure 8 that a maximum value was obtained at a flight Mach number of 1.1 and then at higher flight Mach numbers the diffuser-exit Mach numbers decreased slightly. This apparent decrease in diffuser-exit Mach number may be due to a change in the spanwise velocity profile which was not measured.

The measured velocity and mass flow were somewhat higher than design expectations. This indicates that the losses in the orifice plates were lower than estimated and the back pressure was not quite sufficient. As a result, choking in the entrance occurred over a large range of flight speed. A choking entrance is detrimental to diffuser efficiency, particularly at low flight speeds where the same loss from

choking would become a greater percentage loss in the kinetic energy of the entering air. This accounts for the low values in diffuser efficiency (fig. 9) at a flight speed near $M = 0.75$. At higher flight speeds the efficiency is higher but begins to drop off at velocities greater than $M = 1.2$, possibly because the external losses become greater.

The velocity variation shown in figure 8 is similar to that which would be obtained with the same diffuser on an operating ram jet with fuel-air ratio constant, since the resistance of a combustion chamber operating at constant fuel-air ratio would vary approximately the same as a throttled duct. At operational flight speeds the combustion-chamber velocity levels off and increases only slightly with an increase in flight speed. This small variation of average diffuser-exit velocity is favorable for the operation of ram-jet burners.

Although the diffuser-exit velocity tends to level out at supersonic speeds, the mass flow (fig. 10) shows no tendency in this direction. In fact, the mass flow varies nearly linearly with flight Mach number over the range tested. The increase in density at the diffuser exit with increasing flight Mach number accounts for this variation of mass flow with flight Mach numbers. The curves showing diffuser-exit Mach number, velocity, pressure, and mass flow are all smooth throughout the transonic region indicating the diffusion process to be fairly insensitive to passage through the transonic speed range.

CONCLUSIONS

The diffuser was tested through the transonic speed range and at these speeds the diffusion process was not erratic and the variation of mass flow with flight velocity was smooth. Velocity-distribution curves revealed a large wake from the island as well as a considerable boundary layer from the surface of the shell. If burner operation is impeded by such a nonuniform distribution of velocity at the combustion-chamber entrance, a redesign of the subsonic portion of the diffuser would become necessary. Diffuser efficiency, defined as the percent of kinetic energy recovered, was computed to be 95.5 percent at $M = 1.2$.

Langley Memorial Aeronautical Laboratory
National Advisory Committee for Aeronautics
Langley Field, Va.

REFERENCES

1. Hill, Paul R., and Gammal, A. A.: An Analysis of Ducted-Airfoil Ram Jets for Supersonic Aircraft. NACA RM No. L7I24, 1947.

2. Ferri, Antonio, and Nucci, Louis M.: Preliminary Investigation of a New Type of Supersonic Inlet. NACA RM No. L6J31, 1946.

3. Kantrowitz, Arthur, and Donaldson, Coleman duP.: Preliminary Investigation of Supersonic Diffusers. NACA ACR No. L5D20, 1945.

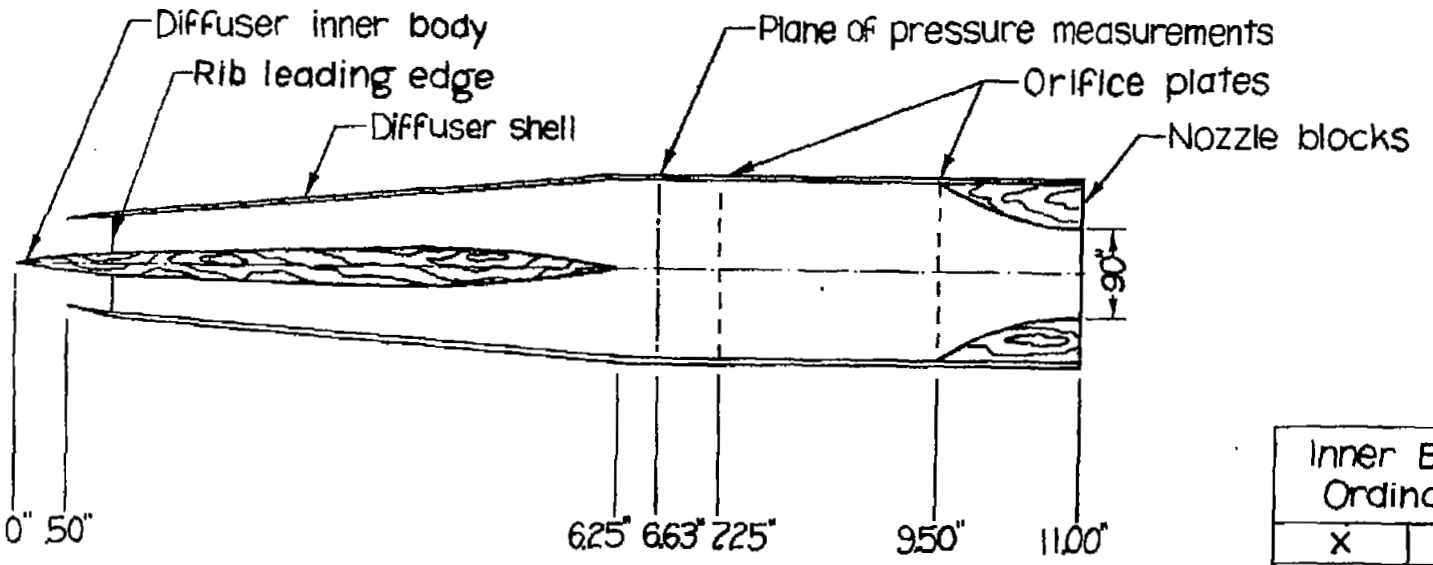

Shell Inner Ordinates	
X	±Y
0.50	0.425
0.63	0.438
0.75	0.450
1.00	0.473
5.75	0.850
6.00	0.865
6.25	0.875

Figure 1.- Ducted airfoil used in diffuser tests.

Inner Body Ordinates	
X	±Y
0.00	0.001
0.25	0.041
0.50	0.079
0.75	0.100
1.00	0.112
1.50	0.130
2.00	0.146
2.50	0.162
3.00	0.176
3.50	0.185
4.00	0.186
4.50	0.175
5.00	0.150
5.50	0.105
6.00	0.040
6.25	0.001

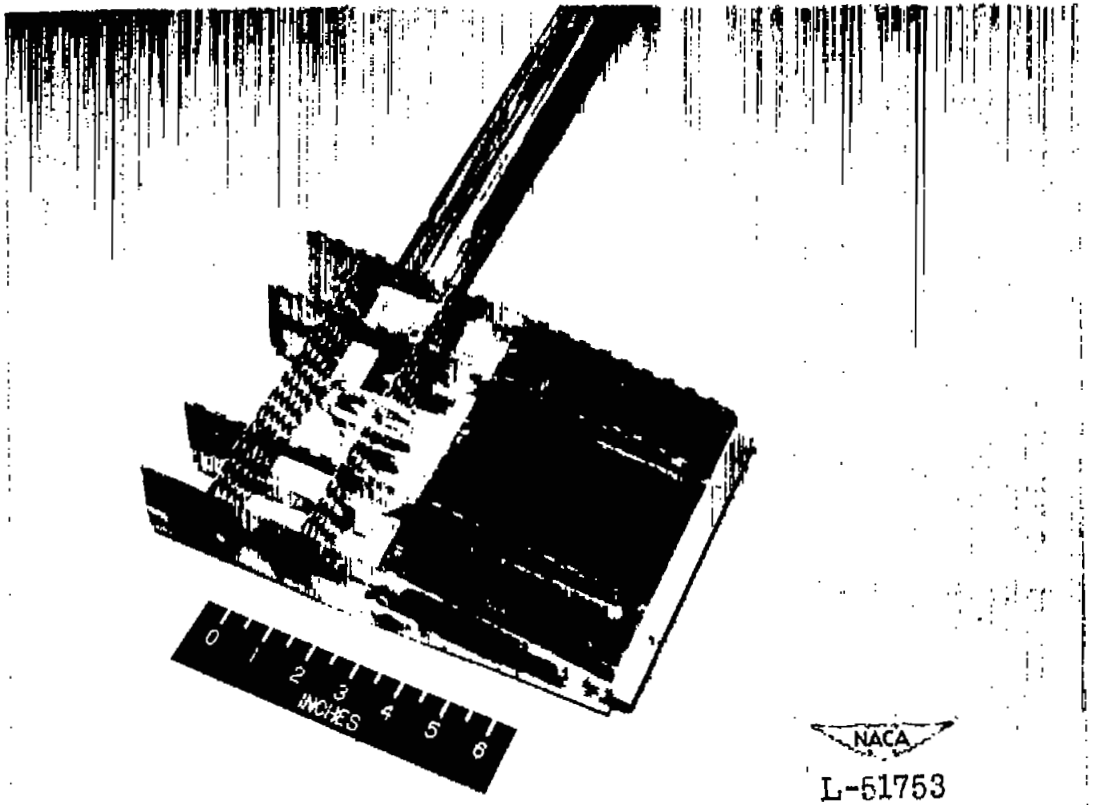

Figure 2.- Construction details of two-dimensional diffuser.

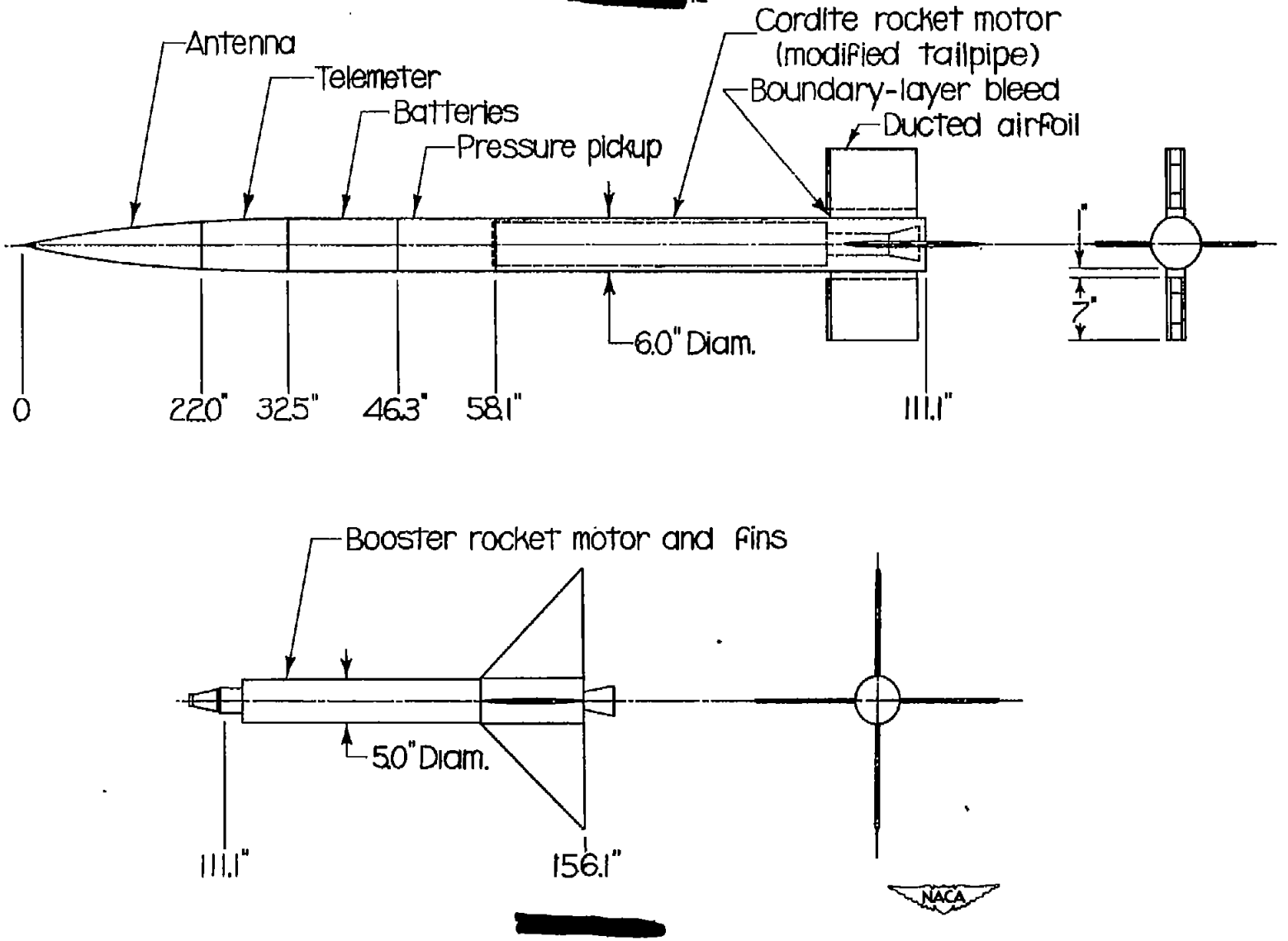

Figure 3.- General arrangement of diffuser test vehicle.

Figure 4.- Diffuser test vehicle assembled on launching rack.

[redacted]L

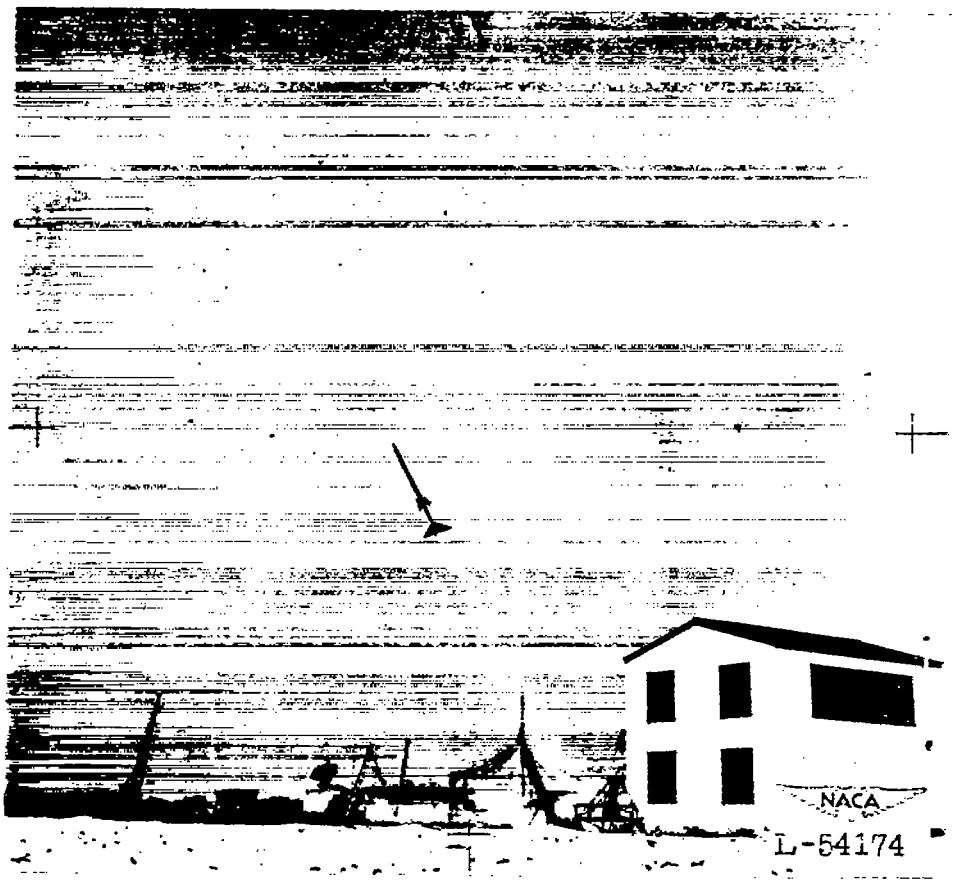

Figure 5.- Launching of diffuser test vehicle.

[redacted]

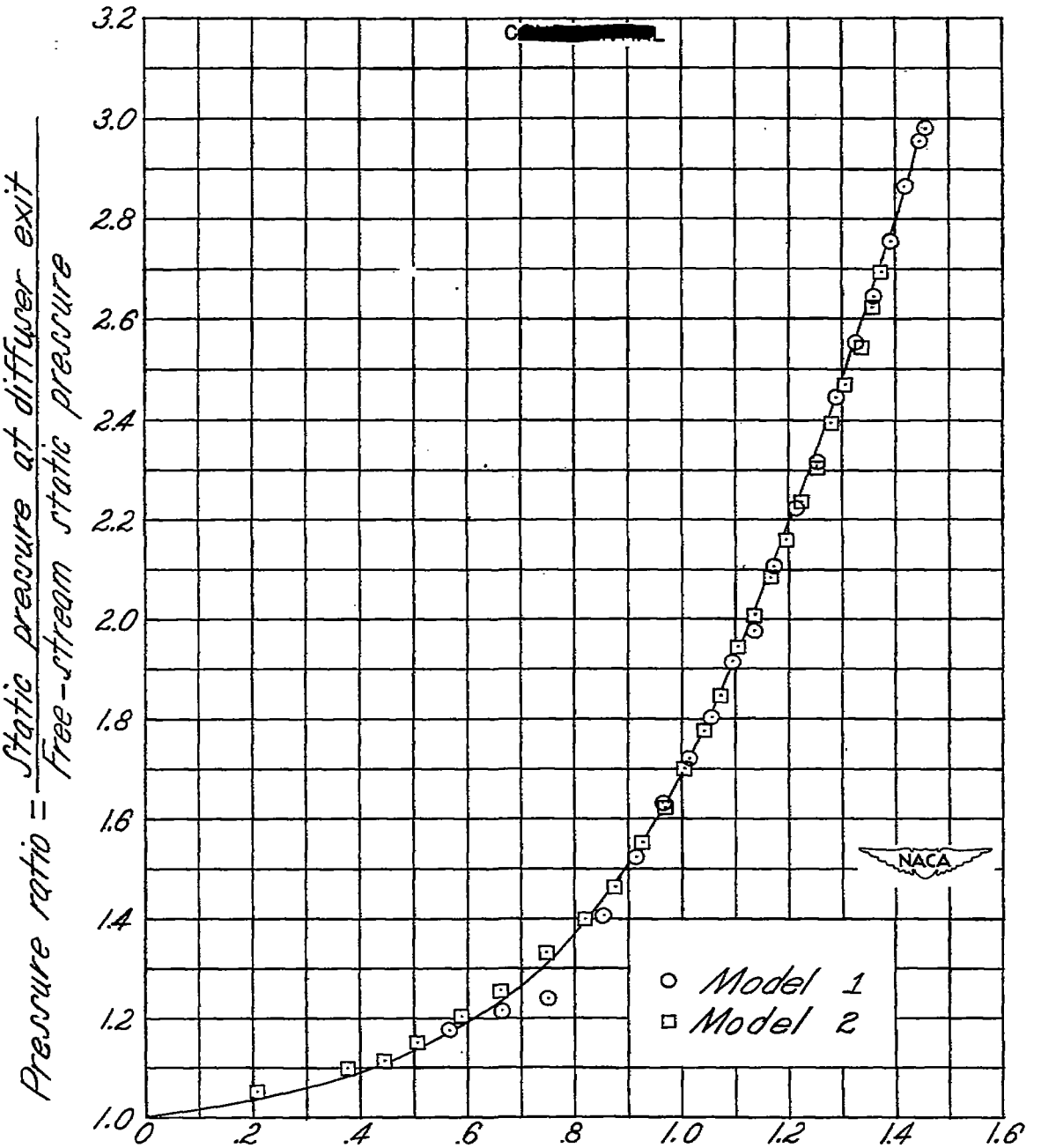

Figure 6. – Pressure ratio against flight Mach number from test of two-dimensional diffuser.

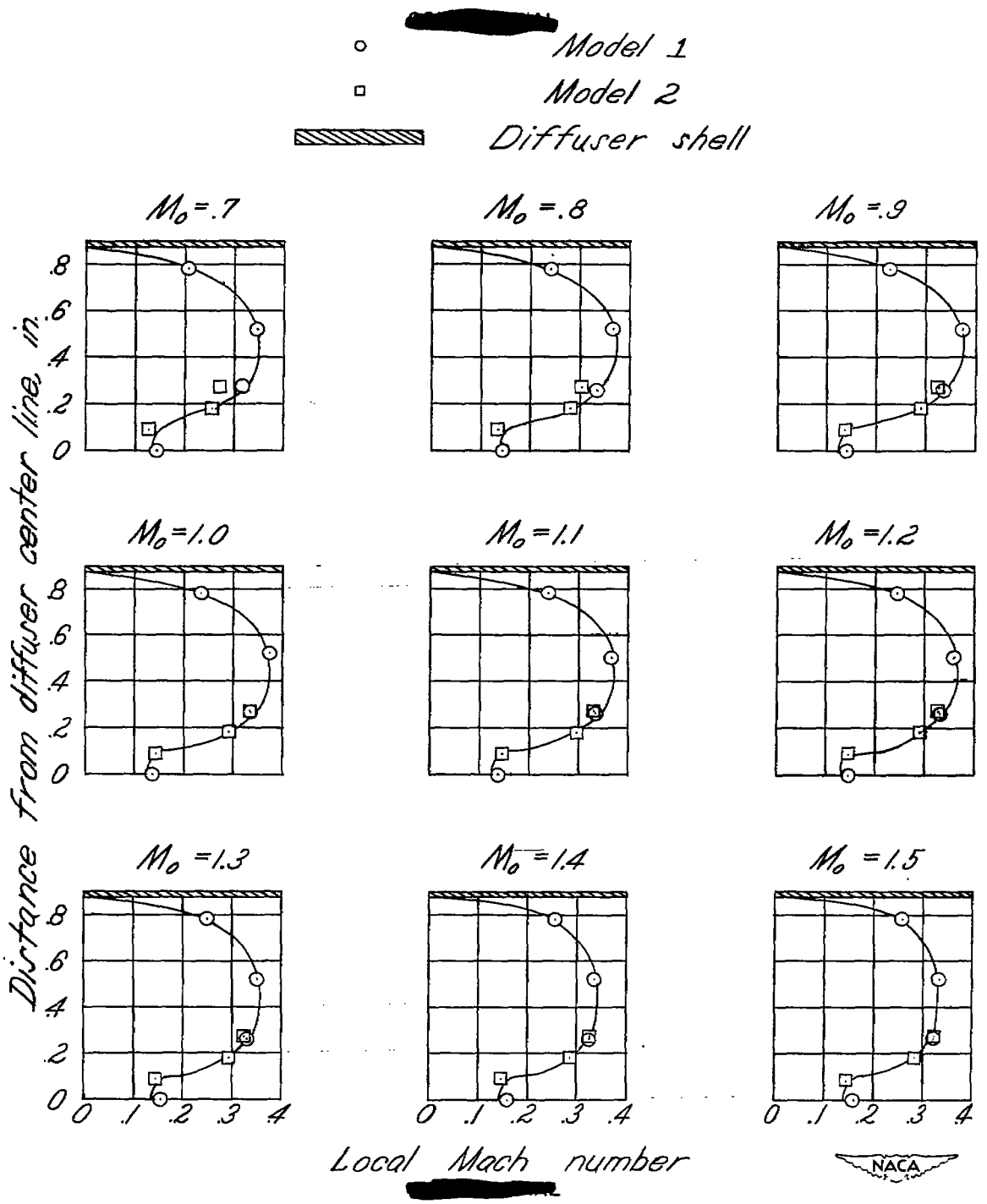

Figure 7.- Velocity distribution at diffuser exit from test of two-dimensional diffuser.

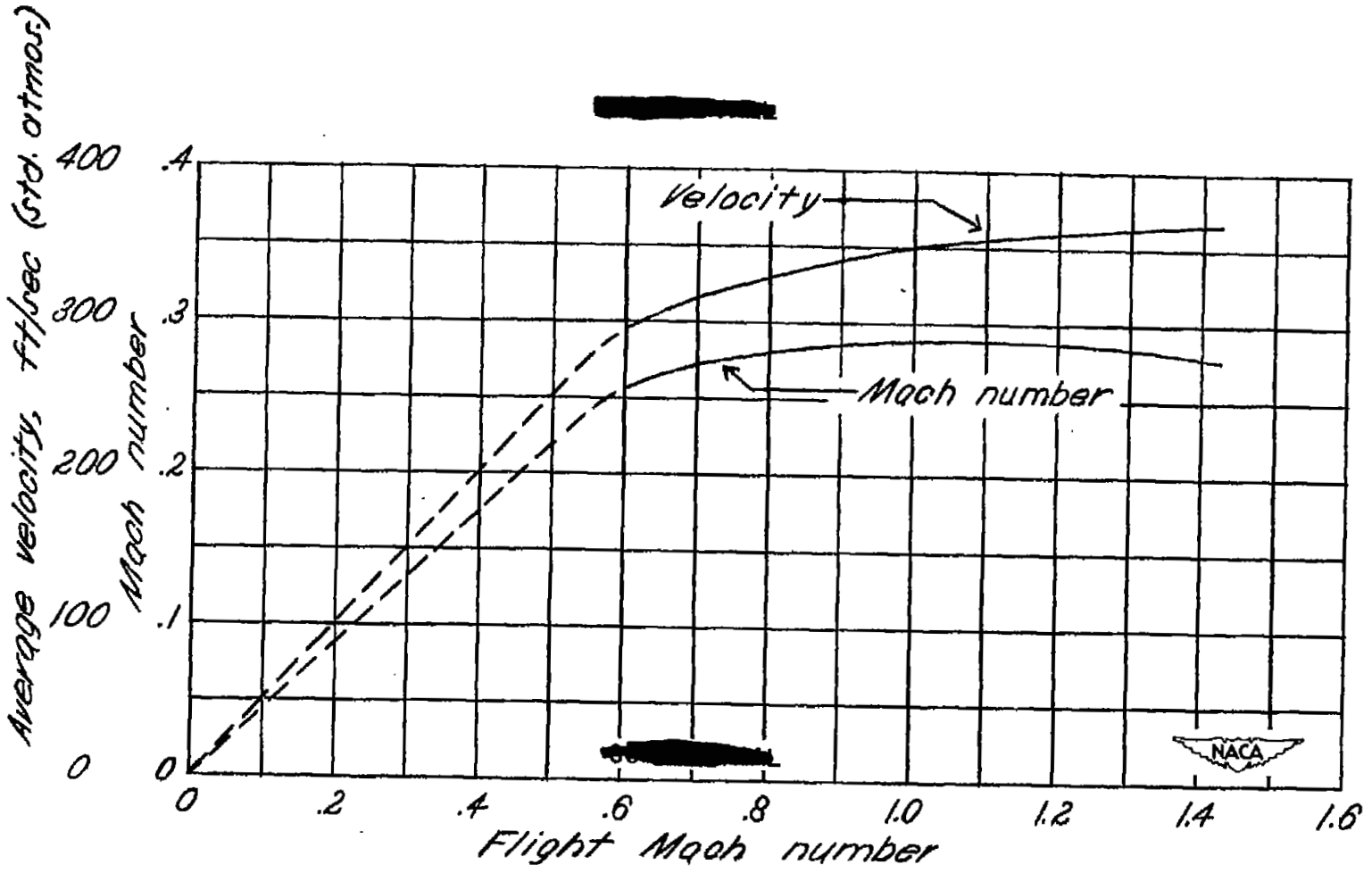

Figure 8.- Average velocity and Mach number at diffuser exit against flight Mach number from test of two-dimensional diffuser.

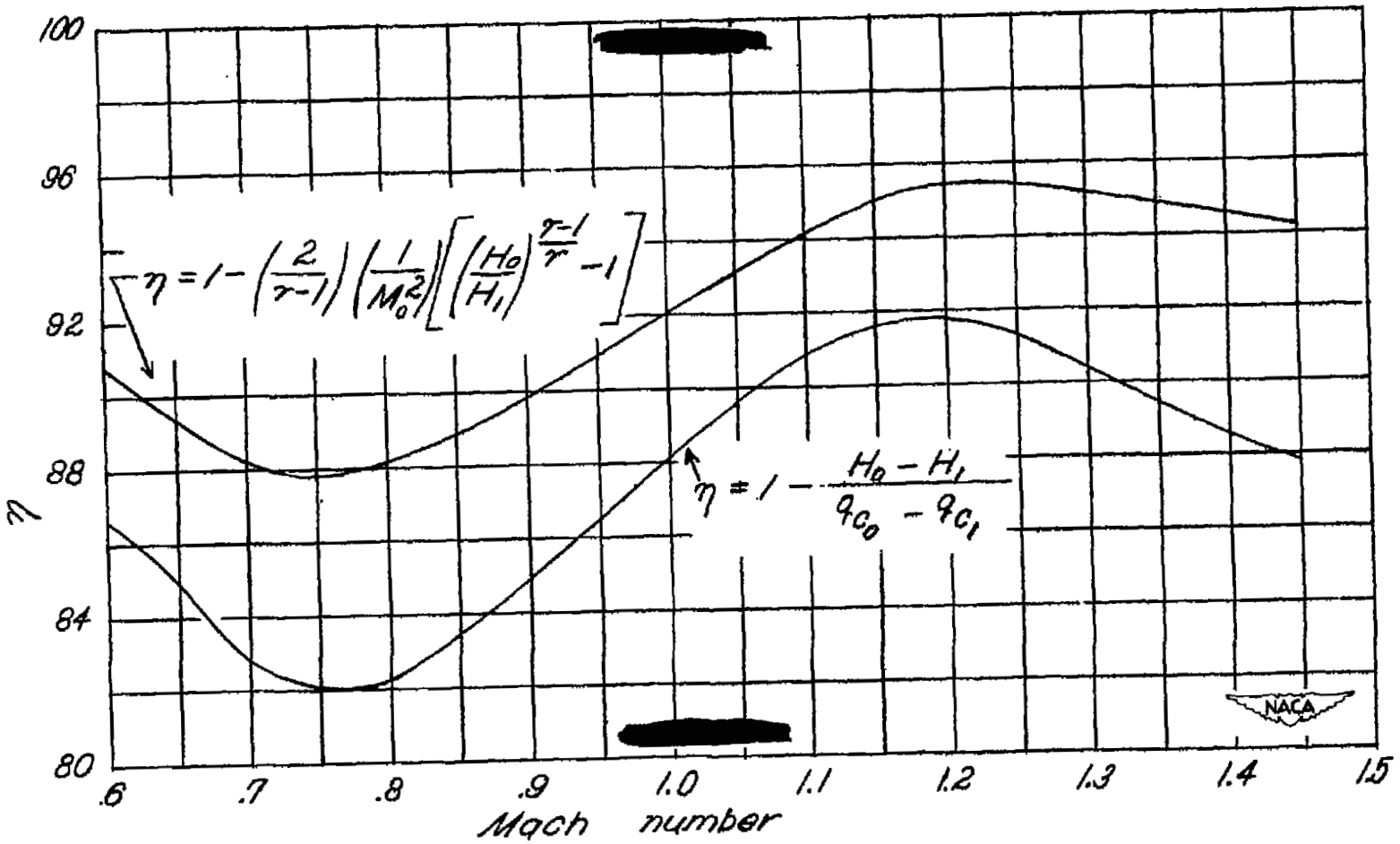

Figure 9. — Diffuser efficiency against flight Mach number from test of two-dimensional diffuser.

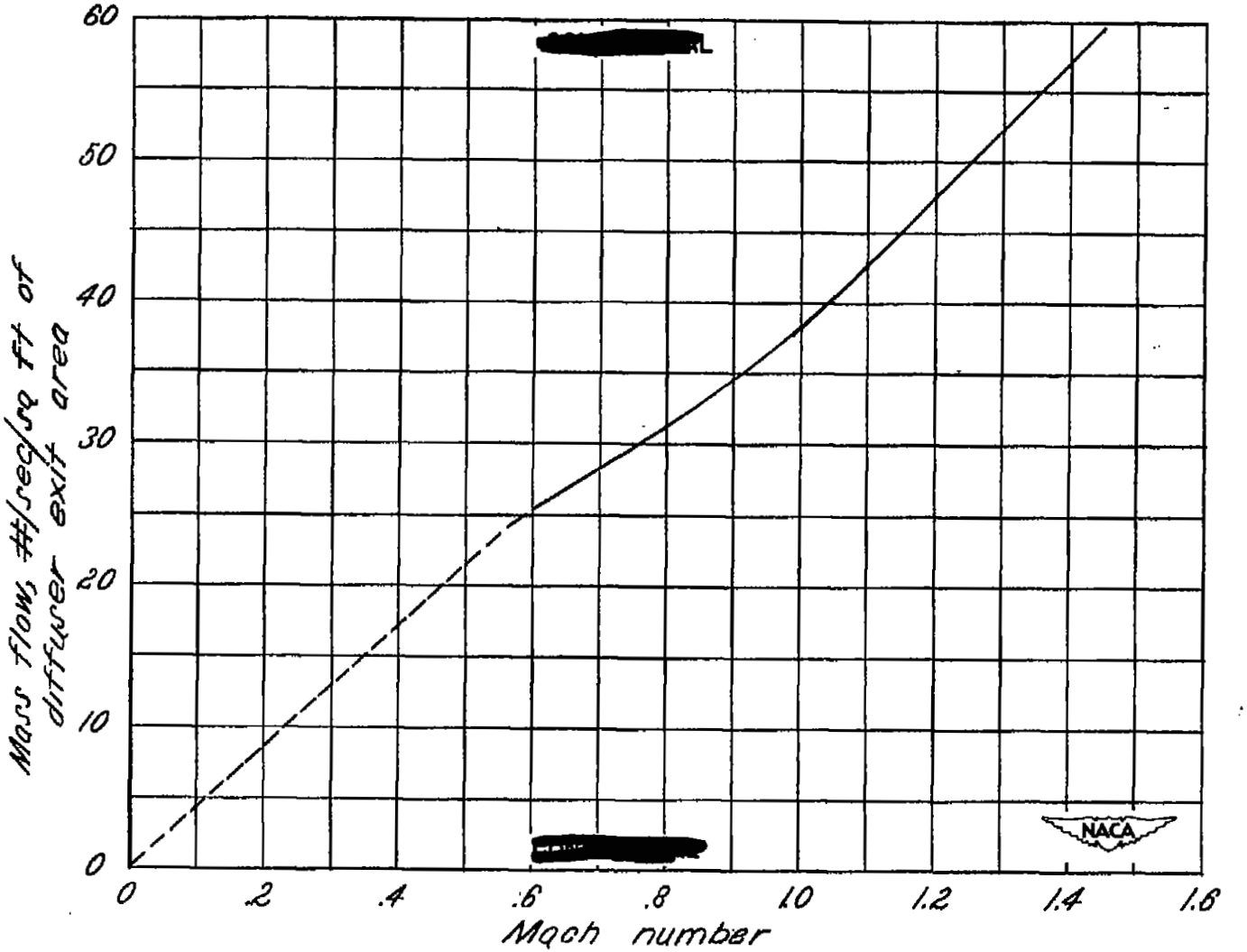

Figure 10.- Mass flow against flight Mach number from test of two-dimensional diffuser.